

# Dissipation induced information scrambling in collision model

Yan Li, Xingli Li, Jiasen Jin\*

*School of Physics, Dalian University of Technology, Dalian 116024, China*

(Dated: January 28, 2022)

In this paper, we present a collision model to stroboscopically simulate the dynamics of information in dissipative systems. In particular, an all-optical scheme is proposed to investigate the information scrambling of bosonic systems with Gaussian environment states. By varying the states of environments, we find that in the presence of dissipation the transient tripartite mutual information of system modes may show negative value signaling the appearance of information scrambling. We also find that dynamical indivisibility based non-Markovianity play dual roles in affecting the dynamics of information.

## I. INTRODUCTION

In closed quantum systems, the locally encoded information can spread into the nonlocal degree of freedom under the unitary transformation, which is referred to as *information scrambling*. The occurrence of information scrambling in the system means that the information of the initial state can not be completely accessed by any local operator after time evolution, which also hints the information delocalization in quantum many-body systems. A quantum system in which the information becomes scrambled can be viewed as a quantum chaotic system: a local operator grows under the time evolution to have large commutators with almost all other operators in the system [1]. The most efficient scrambled system in nature is the black hole. Meanwhile the Sachdev-Ye-Kitaev (SYK) model[2], a toy model of low-dimensional quantum black holes, is also well-known in the field of condensed matter.

A well-known indicator for information scrambling is the out-of-time-order correlator (OTOC) [3–6], which measures the overlap of operators in the dynamics and is intimately related to the Lyapunov exponent. The OTOC is not only widely used to investigate the quantum chaos [7–11], but also plays a dramatic role in characterizing phase transition [12–18] and many-body localization [19–23]. Although the experimental realization of the inverse-time evolution is challenging, the OTOC is still experimentally investigated in trapped ions [24] and nuclear magnetic resonance quantum simulators [25].

The tripartite mutual information (TMI) provides an alternative path to study the information scrambling without the inverse-time evolution [26–29]. In Ref. [1], Hosur *et al.* introduced a map from a unitary quantum channel to a state in a doubled Hilbert space through which the OTOC and TMI are connected. The information scrambling can be characterized by the negative value of TMI. It has already been used to study the weak and strong thermalization [30], information delocalization [31] and quantum frustration [32, 33] in past few decades. Although TMI has the advantage of being operator-independent in witnessing the information scrambling, the exponentially increasing dimension of Hilbert space still limits the further investigations. Meanwhile, an absolutely closed or

isolated system does not exist in reality. As a consequence, studies on the dynamics of information in dissipative systems are desired.

In this paper, we utilize the *collision model* (CM) to tackle those puzzles in open systems. The idea of CM is to represent the system with a particle and the environment with an ensemble of identical particles. The continuous interactions between the system and its environment are thus simulated by a sequence of collision processes. If the system always collides with a fresh environment particle at each step, the information of the system irreversibly flows to the environment which means that the dynamics of the system is Markovian. On the other hand, if the system collides with the environment particles who contain the history of the interactions, the dynamics are considered to be non-Markovian. Apart from the works for investigating the non-Markovian dynamics [34–43], CM has also been used to study the quantum synchronization [44], quantum steering [45], multipartite entanglement generation [46], quantum friction [47] and thermodynamics [48–52], in particular for the quantum thermometry [53, 54]. A comprehensive panorama of the studies on CM can be found in Ref. [55].

Here we propose an experimental feasible scheme to implement the CM in an all-optical network. This allows us to simulate the information dynamics of the continuous-variable system. The all-optical network is consisted of linear optical element such as the beam splitters (BSs). In such scheme, the systems and environment particles are represented by the optical modes in different optical paths. We consider a joint tripartite system composed of an auxiliary mode  $A$  and two system modes  $B$  and  $C$ . Moreover,  $B$  and  $C$  are subjected to individual dissipative channels while mode  $A$  is isolated. The initial information is encoded locally in mode  $B$ . The interactions between different modes are realized through the BSs. By modulating the transmissivities (or reflectivities) of the BSs, the dissipative channels of the system modes can be tuned from the Markovian to the non-Markovian cases. All the input modes are restricted to be the Gaussian states. The non-Markovianity can be quantified by the degree of the violation of dynamical divisibility [56, 57]. We adopt the TMI as the measure of the information scrambling which can be calculated through the symplectic eigenvalues of the so-called covariance matrix.

In the presence of dissipation we find that the information scrambling can be observed before the information completely lost to the environment. Indeed, the non-Markovianity

---

\*Electronic address: [jsjin@dlut.edu.cn](mailto:jsjin@dlut.edu.cn)

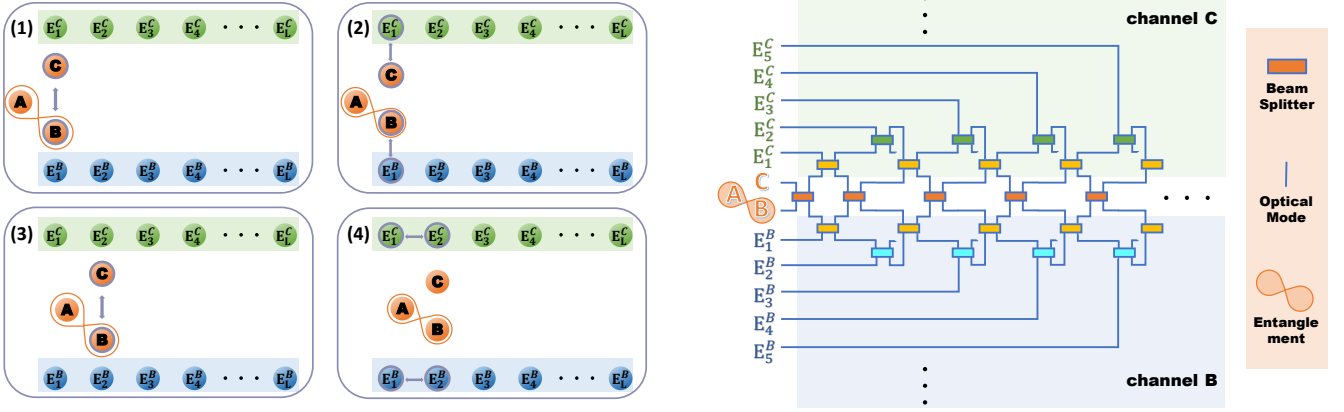


FIG. 1: The left panel is the collision route and the right one is the pictorial illustration of our model. There are two kinds of optical modes, one is system part consisting of  $A$ ,  $B$  and  $C$  of which  $A$  and  $B$  is entangled and  $A$  will not involve in the evolution. And the other is environment part:  $E_j^B$  and  $E_j^C$  which are in the dissipation channel  $B$  and channel  $C$ , respectively. As the collision route shows, the whole process is divided into four parts, and the dynamic process repeats steps (2)-(4) after the step (1) occurs. (1) The collision between  $B$  and  $C$ . (2) The collision between system part and their own environment part. (3) The collision between  $B$  and  $C$ . (4) The collision between environment part. The collision can be realized by BS, as the pictorial illustration shows the orange BS is utilized to mix the two system modes  $B$  and  $C$  of which the transmission angle is written as  $\theta_{ss}$ . The yellow BS is to mix the system mode and environment mode and the transmission is denoted as  $\theta_{se}$ . As for the blue and green BSs are represented the mixture of two environments in their each dissipation Channel  $B$  and  $C$ , besides the transmission angle is written as  $\theta_{ee}^{B(C)}$ .

can affect the time duration of information scrambling, but it is not the key factor for the emergence of information scrambling. We expect that our work may provide a sufficient theoretical support for the experimental studies on the information delocalization in dissipative system.

The paper is organized as follows. In Sec. II, we explain the idea of our CM and the linear optical setup. The mathematical descriptions of the our model are also introduced. In Sec. III, we give the derivation for the degree of the non-Markovianity and TMI based on our CM. In particular, we also present the regime of Markovian and non-Markovian channels in the parameter space. In Sec. IV we show the dynamics of the TMI with different initial states as well as the temperature of environments for both Markovian and non-Markovian cases. We summarize in Sec. V.

## II. COLLISION MODEL

The considered system is comprised of three parts, labeled by  $A$ ,  $B$  and  $C$  which are considered as the auxiliary mode and system modes, respectively. The auxiliary mode  $A$  is isolated while the system modes  $B$  and  $C$  interact to each other and to their individual environments  $E^B$  and  $E^C$ . The dynamics of modes  $B$  and  $C$  can be investigated through the CM in which each system modes is represented by a particle and the environments are represented by ensembles of identical particles. We label the  $j$ -th environment particle of the dissipation channel as  $E_j^{B(C)}$  with  $j = 1, 2, \dots, L-1$ . The intra-system interaction is simulated by the collisions between particles  $B$  and  $C$  while the system-environment interactions are represented by the collisions between the corresponding system and environ-

mental particles. As shown in Fig. 1, our CM works through the following steps,

- (1) The collision between  $B$  and  $C$  takes place.
- (2)  $B$  and  $C$  collide with  $j$ -th environment particles  $E_j^{B(C)}$  individually.
- (3)  $B$  and  $C$  collide with each other again.
- (4) The environment particles  $E_j^{B(C)}$  interact with  $(j+1)$ -th mode  $E_{j+1}^{B(C)}$ .

By repeating steps (2)-(4), the continuous dissipative dynamics of the system can be stroboscopically simulated by a sequence of collisions.

The considered CM can be realized in an all-optical network as shown in Fig. 1. In the all-optical scheme, the system and environment particles can be described by the different optical modes. The interaction between arbitrary two particles can be realized by mixing the corresponding input modes through BSs. The input and output modes are linked by the so-called *scattering matrix* in the following way,

$$\begin{pmatrix} \hat{a}_1^{\text{out}} \\ \hat{a}_2^{\text{out}} \end{pmatrix} = \mathcal{S} \begin{pmatrix} \hat{a}_1^{\text{in}} \\ \hat{a}_2^{\text{in}} \end{pmatrix}, \quad (1)$$

where  $\hat{a}$  and  $\hat{a}^\dagger$  are the annihilation and creation operators of bosonic mode and  $\mathcal{S}$  is the scattering matrix, which is given by the follows,

$$\mathcal{S} = \begin{pmatrix} r & t \\ -t & r \end{pmatrix}. \quad (2)$$

where  $r = \sin \theta$  and  $t = \cos \theta$  are the reflectivity and transmissivity of the BS, and  $\theta \in [0, \pi/2]$  is the tunable parameter. Notice that the reflectivity and transmissivity satisfy  $r^2 + t^2 = 1$ . Basically, there are three types of collisions in our CM: (i) The collision between  $B$  and  $C$ , the scattering matrix is labeled as  $\mathcal{S}_{SS}$  and the parameter is  $\theta_{SS}$ . (ii) The collision between  $B$  ( $C$ ) and its environment mode. We label the scattering matrix as  $\mathcal{S}_{se}$  and the parameter as  $\theta_{se}$ . (iii) The collision between environment modes. The scattering matrix and parameter are  $\mathcal{S}_{EE}$  and  $\theta_{ee}$ , respectively.

In this paper, we restrict the input modes to be Gaussian states. The linear optical elements in the CM always preserve the Gaussianity of the input states. At this sense, the network used here to realize the CM is recognized as Gaussian channels. In order to simulate the time-evolution of the system state, we use the ‘‘temporal’’ index  $L$  to denote the times of collisions in the CM. With the number of the collisions increasing, new optical modes are involved into the scattering matrix at each step. After  $L$ -times collision, the input-output relation of the optical modes is  $[\hat{a}_{E_{L-1}}^{\text{out}}, \hat{a}_{E_{L-2}}^{\text{out}}, \dots, \hat{a}_B^{\text{out}}, \hat{a}_A^{\text{out}}, \hat{a}_C^{\text{out}}, \dots, \hat{a}_{E_{L-2}}^{\text{out}}, \hat{a}_{E_{L-1}}^{\text{out}}]^T = \mathbb{S}(L)[\hat{a}_{E_{L-1}}^{\text{in}}, \hat{a}_{E_{L-2}}^{\text{in}}, \dots, \hat{a}_B^{\text{in}}, \hat{a}_A^{\text{in}}, \hat{a}_C^{\text{in}}, \dots, \hat{a}_{E_{L-2}}^{\text{in}}, \hat{a}_{E_{L-1}}^{\text{in}}]^T$ , here the subscripts  $X = A, B$  and  $C$  represent the corresponding system modes and  $E_j^X$  ( $j = 1, 2, \dots, L-1$ ) denotes the  $j$ -th mode of the environment of system  $X$ . The superscript T denotes the transpose of the vector (or matrix). As shown in Fig. 1, at the first step ( $L = 1$ ), the collision only happens between the system modes, so the total scattering matrix can be constructed by  $\mathbb{S}(1) = \mathcal{S}_{SS}$ . In the next step, the environment modes are involved to collide with the corresponding system modes. Thus the total scattering matrix for  $L = 2$  is  $\mathbb{S}(2) = \mathcal{S}_{SS}\mathcal{S}_{SE_1}\mathcal{S}_{SS}$  (here the subscript of  $\mathcal{S}_{SE_1}$  denotes the scattering matrix linked the system and the first mode of the corresponding environment mode  $E_1^B$  and  $E_1^C$ ). For  $L > 2$ , the total scattering matrix are given as follows

$$\mathbb{S}(L) = \prod_{j=1}^{L-2} (\mathcal{S}_{SS}\mathcal{S}_{SE_{j+1}}\mathcal{S}_{SE_jE_{j+1}}) \mathbb{S}(2). \quad (3)$$

The scattering matrices presented in Eq. (3) are given by

$$\mathcal{S}_{SS} = \begin{pmatrix} \mathbb{I}_{L-1} & 0 & 0 & 0 & 0 \\ 0 & r_{SS} & 0 & t_{SS} & 0 \\ 0 & 0 & 1 & 0 & 0 \\ 0 & -t_{SS} & 0 & r_{SS} & 0 \\ 0 & 0 & 0 & 0 & \mathbb{I}_{L-1} \end{pmatrix}, \quad (4)$$

where  $\mathbb{I}_N$  is the  $N \times N$  identity matrix,

$$\mathcal{S}_{SE_{j+1}} = \begin{pmatrix} \mathbb{I}_{L-j-2} & 0 & 0 & 0 & 0 & 0 & 0 & 0 & 0 \\ 0 & r_{se}^B & 0 & -t_{se}^B & 0 & 0 & 0 & 0 & 0 \\ 0 & 0 & \mathbb{I}_j & 0 & 0 & 0 & 0 & 0 & 0 \\ 0 & t_{se}^B & 0 & r_{se}^B & 0 & 0 & 0 & 0 & 0 \\ 0 & 0 & 0 & 0 & 1 & 0 & 0 & 0 & 0 \\ 0 & 0 & 0 & 0 & 0 & r_{se}^C & 0 & t_{se}^C & 0 \\ 0 & 0 & 0 & 0 & 0 & 0 & \mathbb{I}_j & 0 & 0 \\ 0 & 0 & 0 & 0 & 0 & -t_{se}^C & 0 & r_{se}^C & 0 \\ 0 & 0 & 0 & 0 & 0 & 0 & 0 & 0 & \mathbb{I}_{L-j-2} \end{pmatrix}, \quad (5)$$

where the superscript of the reflectivity (transmissivity) indicates the corresponding dissipation channels, and

$$\mathcal{S}_{E_jE_{j+1}} = \begin{pmatrix} \mathbb{I}_{L-j-2} & 0 & 0 & 0 & 0 & 0 & 0 \\ 0 & r_{ee}^B & -t_{ee}^B & 0 & 0 & 0 & 0 \\ 0 & t_{ee}^B & r_{ee}^B & 0 & 0 & 0 & 0 \\ 0 & 0 & 0 & \mathbb{I}_{2j+1} & 0 & 0 & 0 \\ 0 & 0 & 0 & 0 & r_{ee}^C & t_{ee}^C & 0 \\ 0 & 0 & 0 & 0 & -t_{ee}^C & r_{ee}^C & 0 \\ 0 & 0 & 0 & 0 & 0 & 0 & \mathbb{I}_{L-j-2} \end{pmatrix}. \quad (6)$$

### III. THE FORMALISM

#### A. Characteristic function of Gaussian state

Since the input modes are restricted to be Gaussian states and the channel is Gaussian in the CM, it is convenient to describe the state in characteristic function formalism [58]. For a given quantum state with density matrix  $\rho$ , the corresponding characteristic function is given by  $\chi[\lambda] = \text{tr}[\rho D(\lambda)]$ , where  $D(\lambda)$  is the Weyl displacement operator having the form  $D(\lambda) = \exp(\lambda \hat{a}^\dagger - \lambda^* \hat{a})$ .

In our model, the information is initially encoded in system mode  $B$  through the entanglement between  $B$  and the auxiliary mode  $A$ . The entangled state of modes  $A$  and  $B$  is set to be the two modes squeezed vacuum state (TMSV)  $|\text{TMSV}(\xi)\rangle = \hat{S}(\xi_{AB})|0\rangle_A|0\rangle_B$ . The vector  $|0\rangle$  represents the vacuum state and  $\hat{S}(\xi_{AB})$  is the two-mode squeezing operator given as follows,

$$\hat{S}(\xi_{AB}) = \exp\left(\frac{1}{2}\xi_{AB}^* \hat{a}_A \hat{a}_B - \frac{1}{2}\xi_{AB} \hat{a}_A^\dagger \hat{a}_B^\dagger\right), \quad (7)$$

where  $\xi_{AB} = r_{AB}e^{i\phi_{AB}}$  is the squeezing parameter, and  $r_{AB}$  is the squeezing strength,  $\phi_{AB}$  is the squeezing angle. Meanwhile, the system mode  $C$  is initialized in a generic single mode squeezed vacuum state, which is expressed as  $|\xi_C\rangle = \exp(\frac{1}{2}\xi_C^* \hat{a}_C^2 - \frac{1}{2}\xi_C \hat{a}_C^{\dagger 2})|0\rangle$ . Therefore the joint characteristic function of modes  $A$ ,  $B$  and  $C$  is given by

$$\begin{aligned} \chi_{ABC}^{\text{in}}(\vec{\mu}) &= \exp\left(\frac{\mu_A \mu_B + \mu_A^* \mu_B^*}{2} \sinh \xi_{AB}\right) \\ &\times \exp\left(-\frac{|\mu_A|^2 + |\mu_B|^2}{2} \cosh \xi_{AB}\right) \\ &\times \exp\left(-\frac{|\mu_C|^2}{2} \cosh \xi_C + \frac{e^{-i\phi_C} \mu_C^2 + e^{i\phi_C} (\mu_C^*)^2}{2} \sinh \xi_C\right), \end{aligned} \quad (8)$$

where  $\xi_C = r_C e^{i\phi_C}$  is the squeezing parameter of the system and  $\phi_C$  is the squeezing angle of  $C$  mode. For simplicity, we set the squeezing parameter  $\xi_{AB}$  of the TMSV state to be real.

On the other hand, each environmental mode is in generic single-mode Gaussian state  $\rho_{E_j}(n_{E_j}, \xi_{E_j}, \alpha_{E_j})$ , where  $n_{E_j}$  is the thermal mean photon number,  $\xi_{E_j} = r_{E_j} e^{i\phi_{E_j}}$  is the squeezing parameter of environment mode,  $\phi_{E_j}$  is rotating angle and  $\alpha_{E_j}$  is the complex displacement [59]. The corresponding charac-

teristic function is given as follows,

$$\chi_{E_j}^{\text{in}}(\mu_{E_j}) = \exp \left[ -X_{E_j} |\mu_{E_j}|^2 - \frac{1}{2} (Y_{E_j}^* \mu_{E_j}^2 + Y_{E_j} \mu_{E_j}^{*2}) + Z_{E_j} \mu_{E_j}^* - Z_{E_j}^* \mu_{E_j} \right] \quad (9)$$

where  $X, Y$  and  $Z$  are related to the properties of the Gaussian state. The specific form can be obtained as,

$$\begin{aligned} X_{E_j} &= \left( n_{E_j} + \frac{1}{2} \right) \cosh(2r_{E_j}), \\ Y_{E_j} &= -\left( n_{E_j} + \frac{1}{2} \right) \sinh(2r_{E_j}) e^{i\phi_{E_j}}, \\ Z_{E_j} &= \alpha_{E_j}. \end{aligned} \quad (10)$$

For concise, we have omit the notation of  $B$  and  $C$  in Eqs. (9) and (10). Consequently, the total characteristic function of the system and environmental modes can be described by,

$$\chi_J^{\text{in}}(\vec{\mu}) = \prod_{j=1}^{L-1} \chi_j^{\text{in}}(\vec{\mu}_{E_j^B}) \times \chi_{ABC}^{\text{in}}(\vec{\mu}_{ABC}) \times \prod_{j=1}^{L-1} \chi_j^{\text{in}}(\vec{\mu}_{E_j^C}), \quad (11)$$

where  $\vec{\mu} = [\vec{\mu}_{E^B}, \vec{\mu}_{ABC}, \vec{\mu}_{E^C}]$  is a vector of variables corresponding to the environmental modes  $E^B$ , joint system modes, and environmental modes  $E^C$ , respectively. The reduced characteristic function for the modes of interest can be obtained by simply set the variables associated to the rest modes in  $\vec{\mu}$  to be zero [60]. For instance, by setting  $\vec{\mu} = [0, \dots, 0, \mu_A, \mu_B, \mu_C, 0, \dots, 0]$  in Eq. (11) we could recover the characteristic function for the system modes, i.e. Eq. (8). With the help of the scattering matrix in Eq. (3), the input-output relation for the characteristic functions is given by

$$\chi_J^{\text{out}}(\vec{\mu}) = \chi_J^{\text{in}}(\mathbb{S}^{-1} \vec{\mu}). \quad (12)$$

### B. Non-Markovianity of the dissipative channel

The all-optical network can be considered as a quantum channel that evolve the input states into the output states. A quantum channel is non-Markovian if the memory effect is present. Usually, the non-Markovianity is characterized in two routes: one is based on the information back flow in the time-evolution of a quantum system [61, 62] and the other is based on the degree of the violation of the divisibility of dynamical map [40, 56, 57]. In this work, we will adopt the measure of non-Markovianity for Gaussian channels proposed by Torre *et al.* in Ref. [57].

For Gaussian modes, the covariance matrix is equivalent to the characteristic function in describing the quantum state. In particular, it is very convenient to quantify the measure of non-Markovianity of Gaussian channel and TMI in Gaussian states in terms of covariance matrix. For a single-mode characteristic function, the covariance matrix is the second moment of it and the elements are defined by

$$\sigma_{ml} = \frac{1}{2} \langle \hat{x}_m \hat{x}_l + \hat{x}_m^* \hat{x}_l^* \rangle - \langle \hat{x}_m \rangle \langle \hat{x}_l \rangle, \quad (m, l = 1, 2), \quad (13)$$

where  $\langle \cdot \rangle$  is the expectation value. We have defined  $\hat{x}_1 = (\hat{a}_j + \hat{a}_j^\dagger)/\sqrt{2}$  and  $\hat{x}_2 = (\hat{a}_j - \hat{a}_j^\dagger)/\sqrt{2}i$ . The symmetrically ordered moments can be calculated through the single-mode characteristic function as follows,

$$\text{tr} \left\{ \rho \left[ (\hat{a}_m^\dagger)^p \hat{a}_l^q \right]_{\text{symm}} \right\} = (-1)^q \frac{\partial^{p+q}}{\partial \mu_m^p \partial \mu_l^{*q}} \chi(\mu) \Big|_{\mu=0}. \quad (14)$$

For a  $N$ -mode Gaussian state, the corresponding covariance matrix is  $2N$ -dimensional. According to the Eqs. (12)-(14), one can get following covariance matrix for modes  $A, B$  and  $C$  once the environment states are fixed,

$$\sigma_{ABC} = \begin{pmatrix} \sigma_A & \sigma_{AB} & \sigma_{AC} \\ \sigma_{AB}^\top & \sigma_B & \sigma_{BC} \\ \sigma_{AC}^\top & \sigma_{BC}^\top & \sigma_C \end{pmatrix}, \quad (15)$$

where  $\sigma_x$  ( $x = A, B, C, AB, AC, BC$ ) is a  $2 \times 2$  matrix. The details of those covariance matrices are given in the Appendix.

In terms of the covariance matrix, the input-output relation after  $L$  steps can be reexpressed as  $\sigma^{\text{out},L} = \mathcal{E}_L[\sigma^{\text{in}}]$ . The dynamical map  $\mathcal{E}_L$  is always completely positive and trace-preserving (CPT) and can be formally split in the following manner,

$$\mathcal{E}_L = \Phi_{L,L-1} \circ \mathcal{E}_{L-1}, \quad (16)$$

where the symbol  $\circ$  indicates the composition of the super-operators. When  $\Phi_{L,L-1}$  is CPT for all  $L$ , the dynamics is divisible and Markovian. Conversely, when  $\Phi_{L,L-1}$  is non-CPT for some values of  $L$ , the dynamics is indivisible and non-Markovian. For a generic Gaussian mode, the output covariance matrix takes the following form,

$$\sigma^{\text{out},L} = \mathcal{X}_L \sigma^{\text{in}} \mathcal{X}_L^\top + \mathcal{Y}_L, \quad (17)$$

where  $\mathcal{X}_L$  and  $\mathcal{Y}_L$  are  $2 \times 2$  real matrices. Introduce the matrix

$$\Lambda_L = \mathcal{Y}_{L,L-1} - \frac{i}{2} \Omega + \frac{i}{2} \mathcal{X}_{L,L-1} \Omega \mathcal{X}_{L,L-1}^\top, \quad (18)$$

with  $\mathcal{X}_{L,L-1} = \mathcal{X}_L \mathcal{X}_{L-1}^{-1}$ ,  $\mathcal{Y}_{L,L-1} = \mathcal{Y}_L - \mathcal{X}_{L,L-1} \mathcal{Y}_{L-1} \mathcal{X}_{L,L-1}^\top$ , and  $\Omega = [0, 1; -1, 0]$  being the single mode symplectic matrix. Then the non-Markovianity of the channel basing on the dynamical indivisibility can be quantified by

$$\mathcal{N}(L) = \ln \left( \sum_{j=1}^{L-2} \sum_{k=\pm} \frac{|\lambda_{jk}| - \lambda_{jk}}{2} \right), \quad (19)$$

where  $\lambda_{j,k}$  are the eigenvalues of the matrix  $\Lambda_L$ .

In our CM the dissipative channels for modes  $B$  and  $C$  are assumed to be the same. In this subsection, we will mainly focus on the non-Markovianity of the channel for mode  $C$ . The same results apply to channel of mode  $B$ . We introduce a partial scattering matrix (tilde symbols) associated to mode  $C$  and its environmental modes as the following,

$$\tilde{\mathbb{S}}_E(L) = \prod_{j=1}^{L-2} \left( \tilde{S}_{SE_j} \tilde{S}_{E_{j+1}E_{j+1}} \right) \tilde{S}_{SE_1}, \quad (L \geq 2) \quad (20)$$

where

$$\tilde{S}_{SE_{j+1}} = \begin{pmatrix} r_{se} & 0 & t_{se} & 0 \\ 0 & I_j & 0 & 0 \\ -t_{se} & 0 & r_{se} & 0 \\ 0 & 0 & 0 & I_{L-j-2} \end{pmatrix}, \quad (21)$$

and

$$\tilde{S}_{E_j E_{j+1}} = \begin{pmatrix} I_j & 0 & 0 & 0 \\ 0 & r_{ee} & t_{ee} & 0 \\ 0 & -t_{ee} & r_{ee} & 0 \\ 0 & 0 & 0 & I_{L-j-2} \end{pmatrix}. \quad (22)$$

The partial scattering matrix of channel  $B$  can be obtained by altering the transmissivity  $t_{ee} \rightarrow -t_{ee}$  and  $t_{se} \rightarrow -t_{se}$ .

Therefore, in our specific model the non-Markovianity is calculated by

$$\lambda_{j,\pm} = \ln \left( \left( X_E \pm \frac{1}{2} \sqrt{|Y_E|^2 + 1} \right) \left[ 1 - \frac{c_{1,1}^2(L)}{c_{1,1}^2(L-1)} \right] \right), \quad (23)$$

where  $X_E$  and  $Y_E$  are related to the properties of environmental state as mentioned in Eq. (10) and  $c_{1,1}(L)$  is the element of matrix  $\tilde{S}_E(L)$  at the first row and first column.

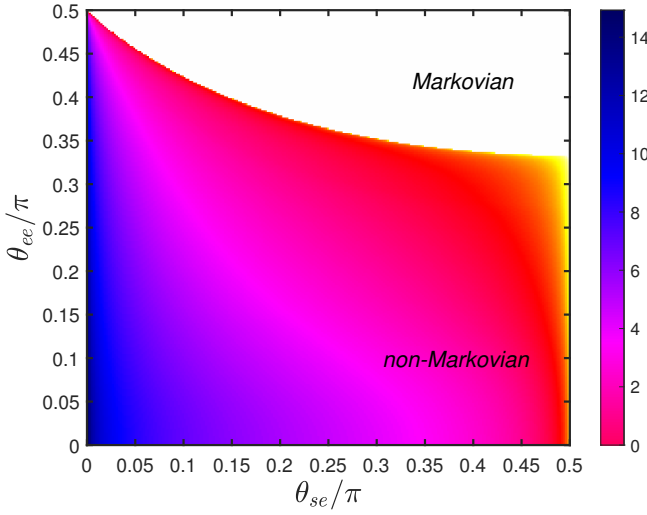


FIG. 2: The non-Markovianity in the  $\theta_{se}$ - $\theta_{ee}$  plane for vacuum environmental states.

In Fig. 2, we show the non-Markovianity in the  $\theta_{ee}$ - $\theta_{se}$  plane for vacuum environmental state. One can see that, by modulating the corresponding transmission angles, the channel can be tuned from the Markovian to non-Markovian. For  $\theta_{ee}/\pi = 0.5$ , the act of environment-environment collision is a complete reflection, thus the lost information is not able to reenter into the system. The dynamics is always Markovian regardless of  $\theta_{se}/\pi$ . In contrast, the small values of  $\theta_{se}$  and  $\theta_{ee}$  mean the high transmissivity of BSs, although the information is likely to leak into the environment, the lost information has large probability to flow back into the system via the environment-environment collisions. The high transmissivity is positive in enhancing the non-Markovianity.

In addition, we find the boundary of Markovian and non-Markovian regions dose not change if the environments are in generic Gaussian states. The degree of the non-Markovianity can be calculated as the following,

$$\mathcal{N}(L) = (2n_E + 1) \cosh(2r_E) \mathcal{N}_{\text{vac}}(L), \quad (24)$$

where  $\mathcal{N}_{\text{vac}}$  is the non-Markovianity of vacuum state.

### C. Tripartite mutual information

In order to witness the delocalization of information during the time-evolution of the state of system, we adopt the TMI as the indicator of information scrambling. For our specific model, the TMI regarding to the auxiliary and system modes is defined as

$$I_3(A : B : C) = I_2(A : B) + I_2(A : C) - I_2(A : BC). \quad (25)$$

In the right-hand side of Eq. (25), the quantities  $I_2$  is the bipartite mutual information (BMI) between the auxiliary mode and the system modes. The BMI quantifies the total correlations between two partition and whose expression of BMI is defined as follows,

$$I_2(A : X) = S(\rho_A) + S(\rho_X) - S(\rho_{AX}), \quad (26)$$

with  $X = B, C$  and  $BC$ . Here  $S(\rho_X) = -\text{tr}[\rho_X \ln \rho_X]$  is the von Neumann entropy of the reduced density matrix for mode  $X$ . Alternatively, the von Neumann entropy for a single-mode Gaussian state  $\rho$  can be obtained by

$$S(\rho) = \sum_{k=1}^N f(\nu_k), \quad (27)$$

where  $f(x) = \left(x + \frac{1}{2}\right) \ln \left(x + \frac{1}{2}\right) - \left(x - \frac{1}{2}\right) \ln \left(x - \frac{1}{2}\right)$  and  $\nu_k$  are the symplectic eigenvalues of the covariance matrix associated to  $\rho$  [63, 64].

The negative value of TMI is a diagnostic of quantum information scrambling. This can be understood as the following. According to Eq. (25), the negative TMI means that the correlation between the auxiliary mode and the joint system modes is more than the sum of correlations between the auxiliary mode to each system mode, namely, the global information about  $A$  embedded in the joint system cannot be accessed by locally measurements on each system mode.

## IV. RESULTS AND DISCUSSIONS

In this section, we will discuss the dynamics of the information in the system modes which interact with their environment. Before that we would consider the dynamics of the joint auxiliary and system modes in the absence of environments. In this case, the joint system (consisted of modes  $A$ ,  $B$  and  $C$ ) is closed and the TMI is always zero during the dynamics governed by the interactions between the system modes. This implies the amount of information about  $A$  encoded in

the joint part  $BC$  is equivalent to those in local parts  $B$  and  $C$ . However, when the system-environment interactions are switched on, the interplay between the unitary evolution and the dissipation will lead to rich phenomena in the dynamics.

### A. Markovian case

In this section, we focus on the Markovian dynamics of TMI. We consider the case that the environments for modes  $B$  and  $C$  are identical. The environmental modes are prepared in the following three types,

1. Vacuum state:  $n_{E_j^{B(C)}} = 0$ ,  $r_{E_j^{B(C)}} = 0$  and  $\alpha_{E_j^{B(C)}} = 0$ ;
2. Squeezed-same state: Squeezed vacuum states with identical squeezing angles  $n_{E_j^{B(C)}} = 0$ ,  $r_{E_j^{B(C)}} \neq 0$ ,  $\phi_{E_j^{B(C)}} = \text{const.}$ ;
3. Squeezed-alternative state: Squeezed vacuum states with the squeezing directions of neighboring mode being perpendicular to each other  $n_{E_j^{B(C)}} = 0$ ,  $r_{E_j^{B(C)}} \neq 0$ ,  $\phi_{E_j^{B(C)}} = \pi$  for odd index  $j$  and  $\phi_{E_j^{B(C)}} = 0$  for even index  $j$ .

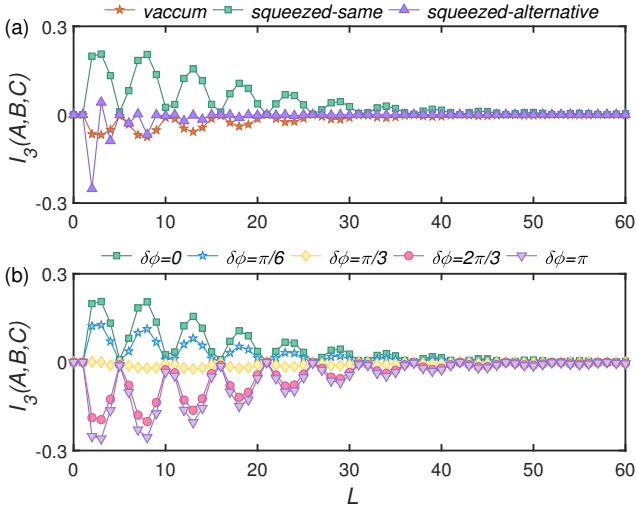


FIG. 3: The  $L$  dependence of TMI for the various environment states. Initially, the auxiliary mode is entangled with system mode  $B$  via two-mode squeezed state with  $\xi_{AB} = 1$ , the system is in squeezed vacuum state with  $\xi_C = 1$ . (a) The environmental modes are in vacuum state, squeezed-same state with all squeezing angle are  $\phi_{E_j^{B(C)}} = 0$ ,  $\forall j$  and squeezed-alternative states with perpendicular squeezing direction between neighbors,  $\phi_{E_j^{B(C)}} = \pi$  for odd index  $j$  and  $\phi_{E_j^{B(C)}} = 0$  for even index  $j$ . The squeezing strengths of the environments parts are  $r_{E_j^{B(C)}} = 0.5$ . (b) For squeezed-same environmental states, the properties of TMI change with phase difference  $\delta\phi = \phi_{E_j^{B(C)}} - \phi_C$ . The tunable parameters of the BSs are  $\theta_{ss} = 0.4\pi$  and  $\theta_{se}^B = \theta_{se}^C = \theta_{ee}^B = \theta_{ee}^C = 0.35\pi$ .

Without loss of generality, we set the parameter of BSs between modes  $B$  and  $C$  to be  $\theta_{ss} = 0.4\pi$ . In Fig. 3, we show

the dynamics of the TMI. The parameters of BSs are set to be  $\theta_{se}^{B(C)} = \theta_{ee}^{B(C)} = 0.35\pi$  to achieve a Markovian channel. One can find that, for any choice of environment state, the TMI always asymptotically approaches to zero in the long-time limit (at large  $L$ ). At the early stage of the evolution, however, the TMI shows damping oscillations. In particular, for the vacuum and squeezed-alternative states, the TMI become negative implying the presence of information scrambling. This can be interpreted as the input vacuum and squeezed states or squeezed states with perpendicular squeezing directions become entangled by passing through the BS.

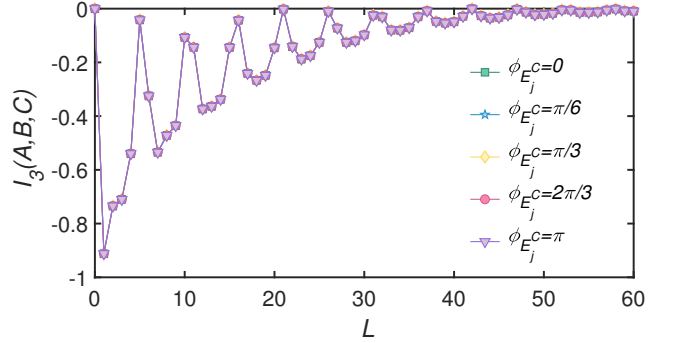


FIG. 4: The  $L$  dependence of TMI for squeezed-same environmental states with different squeezing angles. The system mode  $C$  is in the thermal state with  $n_C = \sinh^2 \xi_C$ . The squeezing parameters of system are  $\xi_{AB} = \xi_C = 1$  and the squeezing strengths of environment are  $r_{E_j^{B(C)}} = 0.5$ . The transmission angles of collisions are  $\theta_{ss} = 0.4\pi$ ,  $\theta_{se}^{B(C)} = \theta_{ee}^{B(C)} = 0.35\pi$ .

From Fig. 3(a), the squeezed-same environmental state seems to always prevent the information being delocalized. Remind that, for this case, mode  $C$  is prepared in the squeezed vacuum state with the same squeezing angle to its environment. In order to investigate the origin of the information scrambling, we investigate the effect of difference between the squeezing angles of mode  $C$  and environment modes. We define the difference as  $\delta\phi = \phi_{E_j^{B(C)}} - \phi_C$  and show the time-evolution of TMI for different  $\delta\phi$  in Fig. 3(b). One can find that as the  $\delta\phi$  increasing there is a crossover from the all positive to negative transient TMI during the time evolution. The minimum negative transient TMI appears when the angle difference is  $\delta\phi = \pi$ , i.e. the squeezing angles of mode  $C$  and environments are perpendicular to each other.

So far we have discussed the case that mode  $C$  is a squeezed state. On the other hand, since mode  $B$  is entangled with the auxiliary mode  $A$  in TMSV state, the reduced state of mode  $B$  is a thermal state with effective photon number being  $\sinh^2 \xi_{AB}$ . We wonder if the unbalanced states in system modes affect the appearance of information scrambling. With this goal in mind, we set mode  $C$  to be in a thermal state that is identical to the reduced state of mode  $B$  and investigate the time-evolution of TMI. The result is shown in Fig. 4. One can see that even if the states of modes  $B$  and  $C$  are effectively identical to each other and will not entangled through the BS, the transient TMI may be negative during the evolution implying that dissipation is responsible for the informa-

tion scrambling. In addition, we find that squeezing angle of environmental states does not change the value of TMI.

### B. Non-Markovian case

In this section, we will discuss the effect of non-Markovianity of the channels on information scrambling. As mentioned in Sec. III B, the non-Markovianity of the channels can be switched on by tuning the parameters  $\theta_{se}$  and  $\theta_{ee}$  of BSs. Once the parameter  $\theta_{se}$  is fixed, the degree of non-Markovianity will decrease with  $\theta_{ee}$  increasing and vice versa. Here we set the system mode  $C$  to be in squeezed vacuum state and the environmental modes to be in the vacuum state.

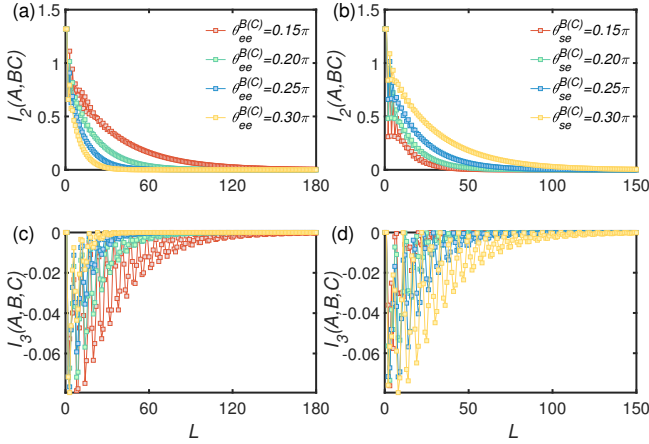


FIG. 5: The  $L$  dependence of BMI and TMI for the states of the dissipation channel being the vacuum state with  $\theta_{ss} = 0.4\pi$ . (a) and (c) is the dynamics of BMI and TMI with different transmission angle  $\theta_{ee}^{B(C)}$  when  $\theta_{se}^{B(C)} = 0.25\pi$ . (b) and (d) is the dynamic of BMI and TMI with different  $\theta_{se}^{B(C)}$  when  $\theta_{ee}^{B(C)} = 0.2\pi$ .

In Fig. 5 we show the time-evolution of BMI and TMI for fixed  $\theta_{se}$  and  $\theta_{ee}$ . From Fig. 5(a) and (c), one can find that with  $\theta_{ee}$  increasing the decay of BMI between the auxiliary mode and joint system modes become faster meaning that the encoded information is leaking out into the environment. This is because the larger  $\theta_{ee}$  the less information gained by the new environment mode through environment-environment collision, and consequently the less information flowing back to the system. Nevertheless the information still has the possibility to flow back to the system which is revealed by the nonmonotonic decay of BMI at the early stage in the time-evolution. Correspondingly, the TMI also oscillates before the encoded information in the system modes being completely lost.

In contrast, as shown in Fig.5(b), when the parameter  $\theta_{ee}$  is fixed, the decay rate of BMI becomes larger as  $\theta_{se}$  decreasing. The behavior of TMI shows the similar trends. It is counterintuitive that the strong non-Markovianity speeds up the leaking of information. We interpret this point by considering that non-Markovianity is measured by the indivisibility of dissipative channel. Indeed, the negative eigenvalues become smaller (or say the absolute value become larger) as  $\theta_{se}$  decreasing

which indicate the strong non-Markovianity, meanwhile, the reflectivity of BS between  $C$  and environment modes is however getting smaller which facilitate the lost of information from system mode.

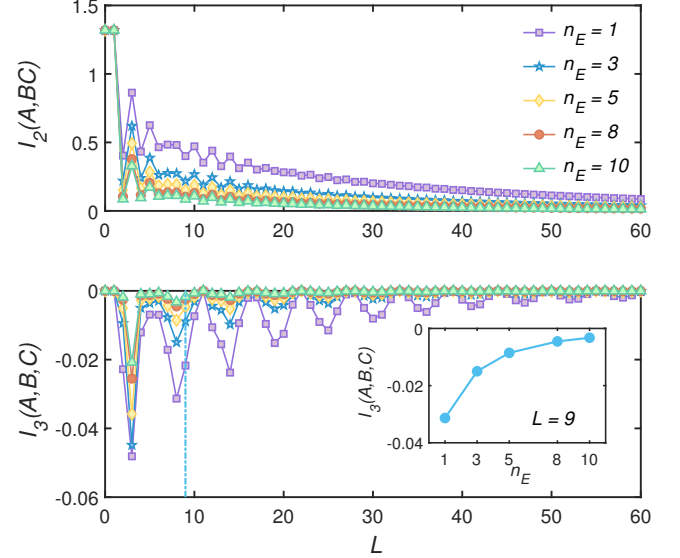


FIG. 6: The  $L$  dependence of BMI and TMI with the environment part being different thermal states with the thermal mean number  $n$  in fixed transmission angle  $\theta_{se}^{B(C)} = 0.3\pi$  and  $\theta_{ee}^{B(C)} = 0.15\pi$ . Besides, the transmission angle  $\theta_{ss} = 0.4\pi$ .

Another way to tune the degree of non-Markovianity of the channel is to change the states of environmental modes. According to Eq.(24), the non-Markovianity will be amplified as the effective photon number of environmental thermal state increasing. In Fig. 6, we show the time-evolution of BMI and TMI for different  $n_E$ . It turns out that the transient value of both BMI and TMI is proportional to the effective photon number as shown in the inset of Fig. 6(b). In this case, the non-Markovianity only quantitatively modifies the time-evolution of information.

We end this section by concluding that the degree of non-Markovianity of dissipative channel can indeed affect the dynamics of the information, but there is not an explicit relationship between the presence of non-Markovianity and occurrence of information scrambling in our CM.

## V. SUMMARY

In summary, we have proposed an all-optical scheme to simulate the CM. By virtue of the characteristic function formalism, we were able to deal with a large number of bosonic modes and take the interactions between different modes into account. We have considered the cases that system and environmental modes are in various Gaussian states. We have investigated the stroboscopic evolution of information, which is initially encoded the one of the system mode via entangling it with an auxiliary mode, in a three-mode system in the presence of dissipations.

By varying the parameters of BSs in the all-optical network, the dissipative channel can be tuned from Markovian to non-Markovian. In the Markovian case, if system mode is prepared in the squeezed vacuum state, we found that the vacuum and squeezed-alternative environmental states may scramble the information during the dynamics. While the environment being squeezed-same state, there will be a crossover from the absence to presence of information scrambling by changing the difference of squeezing angles between system modes and environmental modes. We have also investigated the case that two system modes are effectively equivalent in terms of thermal states. The results reveal that the occurrence of information scrambling is induced by the dissipation instead of unbalanced system states. In the non-Markovian case, we found that the non-Markovianity can indeed affect the time-evolution of information, however there is not an explicit relationship between the non-Markovianity of the channels and the appearance of information scrambling in our CM.

Finally, with the benefits of high stability, arbitrary control of transmissivity, modular nature, and flexible scalability, the all-optical platform can be utilized to simulate the Gaussian boson sampling [65–68], Anderson localization [69], quantum walk [70], and quantum state transfer [71, 72]. Recently, temporal steering has been utilized as another potential candidate for witnessing information scrambling [73], the experimental realization of temporal steering in the framework of CM is an intriguing perspective..

### Acknowledgments

This work is supported by National Natural Science Foundation of China under Grant No. 11975064.

### APPENDIX

In this appendix, we show the specific forms of Eq.(15) where the matrix elements  $\sigma_X$  is the two-dimensional matrices. The detailed forms of the diagonal matrix elements are given as following,

$$\sigma_A = \frac{1}{2} \begin{pmatrix} \cosh(\xi_{AB}) & 0 \\ 0 & \cosh(\xi_{AB}) \end{pmatrix}, \quad (28)$$

$$\sigma_B = \begin{pmatrix} \alpha^B + \beta^B & \gamma^B \\ \gamma^B & \alpha^B - \beta^B \end{pmatrix}, \quad (29)$$

$$\sigma_C = \begin{pmatrix} \alpha^C + \beta^C & \gamma^C \\ \gamma^C & \alpha^C - \beta^C \end{pmatrix}, \quad (30)$$

the specific forms of the elements in Eq.(29) and Eq.(30) are

$$\begin{aligned} \alpha^{B(C)} &= \frac{1}{2} \left( \cosh(\xi_{AB}) |c_{L,k}|^2 + \cosh(\xi_C) |c_{L+2,k}|^2 \right) \\ &+ \frac{1}{2} \left[ \sum_{w=1}^{L-1} \left( \cosh(2r_{E_w^B}) + \left( n_{E_w^B} + \frac{1}{2} \right) \right) |c_{w,k}|^2 \right] \\ &+ \frac{1}{2} \left[ \sum_{z=L+3}^{2L+1} \left( \cosh(2r_{E_{z-L-2}^C}) + \left( n_{E_{z-L-2}^C} + \frac{1}{2} \right) \right) |c_{z,k}|^2 \right] \\ \beta^{B(C)} &= \frac{1}{4} \sinh(\xi_C) (c_{L+2,k}^{*2} + c_{L+2,k}^2) \\ &+ \frac{1}{2} \Re \left( \sum_{w=1}^{L-1} \sinh(2r_{E_w^B}) e^{i\phi_{E_w^B}} c_{w,k}^{*2} + \sum_{z=L+3}^{2L+1} \sinh(2r_{E_z^C}) e^{i\phi_{E_z^C}} c_{z,k}^{*2} \right) \\ \gamma^{B(C)} &= \frac{1}{4i} \sinh(\xi_C) (c_{L+2,k}^{*2} - c_{L+2,k}^2) \\ &+ \frac{1}{2} \Im \left( \sum_{w=1}^{L-1} \sinh(2r_{E_w^B}) e^{i\phi_{E_w^B}} c_{w,k}^{*2} + \sum_{z=L+3}^{2L+1} \sinh(2r_{E_{z-L-2}^C}) e^{i\phi_{E_{z-L-2}^C}} c_{z,k}^{*2} \right) \end{aligned}$$

where  $c_{i,j}$  expresses the matrix element in the  $i$ -th row and  $j$ -th column of  $\mathbb{S}^{-1}(L)$ , and the matrix is given in the main text. The subscript  $k$  varies with subscript  $B(C)$  of  $\alpha^{B(C)}$ ,  $\beta^{B(C)}$  and  $\gamma^{B(C)}$ ,  $k = L$  is for subscript  $B$  and  $k = L + 2$  is for subscript  $C$ . Recall the main text,  $\xi_{AB}$  and  $\xi_C$  are the squeezed parameters of the joint system  $AB$  and system part  $C$ , respectively. For the environment part,  $n_{E_j^{B(C)}}$ ,  $r_{E_j^{B(C)}}$  and  $\phi_{E_j^{B(C)}}$  are the thermal mean photon number, squeezed strength and squeezed angle of the  $j$ -th environment state in the dissipation channel  $B(C)$ .

Meanwhile, the off-diagonal matrix elements are governed in the following form,

$$\sigma_{AB} = \frac{\sinh(\xi_{AB})}{2} \begin{pmatrix} \Re(c_{L,L}^*) & \Im(c_{L,L}^*) \\ \Im(c_{L,L}^*) & -\Re(c_{L,L}^*) \end{pmatrix}, \quad (31)$$

$$\sigma_{AC} = \frac{\sinh(\xi_{AB})}{2} \begin{pmatrix} \Re(c_{L,L+2}^*) & \Im(c_{L,L+2}^*) \\ \Im(c_{L,L+2}^*) & -\Re(c_{L,L+2}^*) \end{pmatrix}, \quad (32)$$

$$\sigma_{BC} = \frac{1}{2} \begin{pmatrix} K + M & P + Q \\ P - Q & K + M \end{pmatrix}, \quad (33)$$

with the matrix elements in a general form,

$$\begin{aligned}
\mathbf{K} &= \Re \left( \cosh(\xi_{AB}) c_{L,L} c_{L,L+2}^* + \cosh(\xi_C) c_{L+2,L} c_{L+2,L+2}^* \right) \\
&+ \Re \left[ \sum_{w=1}^{L-1} \left( \cosh(2r_{E_w^B}) + \left( n_{E_w^B} + \frac{1}{2} \right) \right) c_{w,L} c_{w,L+2}^* \right] \\
&+ \Re \left[ \sum_{z=L+3}^{2L+1} \left( \cosh(2r_{E_{z-L-2}^C}) + \left( n_{E_{z-L-2}^C} + \frac{1}{2} \right) \right) c_{z,L} c_{z,L+2}^* \right] \\
\mathbf{M} &= \sinh(\xi_C) \Re \left( c_{L+2,L}^* c_{L+2,L+2}^* \right) \\
&+ \Re \left( \sum_{w=1}^{L-1} \sinh(2r_{E_w^B}) e^{i\phi_{E_w^B}} c_{w,L}^* c_{w,L+2}^* + \sum_{z=L+3}^{2L+1} \sinh(2r_{E_{z-L-2}^C}) e^{i\phi_{E_{z-L-2}^C}} c_{z,L}^* c_{z,L+2}^* \right) \\
\mathbf{P} &= \sinh(\xi_C) \Im \left( c_{L+2,L}^* c_{L+2,L+2}^* \right) \\
&+ \Im \left( \sum_{w=1}^{L-1} \sinh(2r_{E_w^B}) e^{i\phi_{E_w^B}} c_{w,L}^* c_{w,L+2}^* + \sum_{z=L+3}^{2L+1} \sinh(2r_{E_{z-L-2}^C}) e^{i\phi_{E_{z-L-2}^C}} c_{z,L}^* c_{z,L+2}^* \right) \\
\mathbf{Q} &= \frac{1}{2} \Im \left( \cosh(\xi_{AB}) c_{L,L} c_{L,L+2}^* + \cosh(\xi_C) c_{L+2,L} c_{L+2,L+2}^* \right) \\
&+ \frac{1}{2} \Im \left[ \sum_{w=1}^{L-1} \left( \cosh(2r_{E_w^B}) + \left( n_{E_w^B} + \frac{1}{2} \right) \right) c_{w,L} c_{w,L+2}^* \right] \\
&+ \frac{1}{2} \Im \left[ \sum_{z=L+3}^{2L+1} \left( \cosh(2r_{E_{z-L-2}^C}) + \left( n_{E_{z-L-2}^C} + \frac{1}{2} \right) \right) c_{z,L} c_{z,L+2}^* \right]
\end{aligned}$$

- 
- [1] P. Hosur, X.-L. Qi, D. A. Roberts, and B. Yoshida, Chaos in quantum channels, *J. High Energy Phys.* **02** 004 (2016).
- [2] S. Sachdev and J. Ye, Gapless spin-fluid ground state in a random quantum Heisenberg magnet, *Phys. Rev. Lett.* **70**, 3339 (1993).
- [3] B. Swingle, G. Bentsen, Monika S. -S. and P. Hayden, Measuring the scrambling of quantum information, *Phys. Rev. A* **94** 040302(R) (2016).
- [4] C. B. Dağ and L. -M. Duan, Detection of out-of-time-order correlators and information scrambling in cold atoms: Ladder-XX model, *Phys. Rev. A* **99**, 052322 (2019).
- [5] J. R. G. Alonso, N. Y. Halpern, and J. Dressel, Out-of-Time-Ordered-Correlator Quasiprobabilities Robustly Witness Scrambling, *Phys. Rev. Lett.* **122**, 040404 (2019).
- [6] K. A. Landsman, C. Figgatt, T. Schuster, N. M. Linke, B. Yoshida, N. Y. Yao, and C. Monroe, Verified quantum information scrambling, *Nature* **567**, 61 (2019).
- [7] J. Maldacena, S. H. Shenker, and D. Stanford, A bound on chaos, *J. High Energy Phys.* **08** 106 (2016).
- [8] D. A. Roberts and D. Stanford, Diagnosing Chaos Using Four-Point Functions in Two-Dimensional Conformal Field Theory, *Phys. Rev. Lett.* **115**, 131603 (2015).
- [9] J. Polchinski and V. Rosenhaus, The spectrum in the SachdevYe-Kitaev model, *J. High Energy Phys.* **04** 001 (2016).
- [10] M. Mezei and D. Stanford, On entanglement spreading in chaotic systems, *J. High Energy Phys.* **05** 065 (2017).
- [11] D. A. Roberts and B. Yoshida, Chaos and complexity by design, *J. High Energy Phys.* **04** 121 (2017).
- [12] H. Shen, P. Zhang, R. Fan, and H. Zhai, Out-of-time-order correlation at a quantum phase transition, *Phys. Rev. B* **96**, 054503 (2017).
- [13] M. Heyl, F. Pollmann, and B. Dóra, Detecting Equilibrium and Dynamical Quantum Phase Transitions in Ising Chains via Out-of-Time-Ordered Correlators, *Phys. Rev. Lett.* **121**, 016801 (2018).
- [14] Q. Wang and F. Pérez-Bernal, Probing an excited-state quantum phase transition in a quantum many-body system via an out-of-time-order correlator, *Phys. Rev. A* **100**, 062113 (2019).
- [15] C. B. Dağ, K. Sun, and L.-M. Duan, Detection of Quantum Phase Via Out-of-Time-Order Correlators, *Phys. Rev. Lett.* **123**, 140602 (2019).
- [16] S. Sahu, S. Xu, and B. Swingle, Scrambling dynamics across a thermalization-localization quantum phase transition, *Phys. Rev. Lett.* **123**, 165902 (2019).
- [17] S. Choi, Y. Bao, X. -L. Qi, and Ehud Altman, Quantum Error Correction in Scrambling Dynamics and Measurement-Induced Phase Transition, *Phys. Rev. Lett.* **125**, 030505 (2020).
- [18] R. K. Shukla, G. K. Naik, and S. K. Mishra, Out-of-time-order correlation and detection of phase structure in Floquet transverse Ising spin system, *EPL*, **132**, 04. (2021).
- [19] Y. Huang, Y.-L. Zhang, and X. Chen, Out-of-time-ordered correlators in many-body localized systems, *Ann. Phys.* **529**, 1600318 (2016).
- [20] R. Fan, P. Zhang, H. Shen, and H. Zhai, Out-of-time-order correlation for many-body localization, *Sci. Bull.* **62**, 707 (2017).
- [21] X. Chen, T. Zhou, D. A. Huse, and E. Fradkin, Out-of-time-order correlations in many-body localized and thermal phases, *Ann. Phys.* **529**, 1600332 (2016).
- [22] R.-Q. He and Z.-Y. Lu, Characterizing many-body localization by out-of-time-ordered correlation, *Phys. Rev. B* **95**, 054201 (2017).
- [23] B. Swingle and D. Chowdhury, Slow scrambling in disordered

- quantum systems, *Phys. Rev. B* **95**, 060201(R) (2017).
- [24] M. Gärtner, J. G. Bohnet, A. Safavi-Naini, M. L. Wall, J. J. Bollinger, and A. M. Rey, Measuring out-of-time-order correlations and multiple quantum spectra in a trapped-ion quantum magnet, *Nat. Phys.* **13**, 781 (2017).
- [25] J. Li, R. Fan, H. Wang, B. Ye, B. Zeng, H. Zhai, X. Peng, and J. Du, Measuring Out-of-Time-Order Correlators on a Nuclear Magnetic Resonance Quantum Simulator, *Phys. Rev. X* **7**, 031011 (2017).
- [26] E. Iyoda and T. Sagawa, Scrambling of quantum information in quantum many-body systems, *Phys. Rev. A* **97**, 042330 (2018).
- [27] O. Schnaack, N. Bölter, S. Paeckel, S. R. Manmana, S. Kehrein, and M. Schmitt, Tripartite information, scrambling, and the role of Hilbert space partitioning in quantum lattice models, *Phys. Rev. B* **100**, 224302 (2019).
- [28] H. Shen, P. Zhang, Y. -Z. You, and H. Zhai, Information scrambling in quantum neural networks, *Phys. Rev. Lett.* **124**, 200504 (2020).
- [29] D. Wanisch, and S. Fritzsche, Delocalization of quantum information in long-range interacting systems, *Phys. Rev. A* **104**, 042409 (2021).
- [30] Z. -H. Sun, J. Cui, and H. Fan, Quantum information scrambling in the presence of weak and strong thermalization, *Phys. Rev. A* **104**, 022405.
- [31] D. Wanisch and S. Fritzsche, Delocalization of quantum information in long-range interacting systems, *Phys. Rev. A* **104**, 042409 (2021).
- [32] H. Matsuda, Physical nature of higher-order mutual information: Intrinsic correlations and frustration, *Phys. Rev. E* **62**, 3096 (2000).
- [33] H. Matsuda, Information theoretic characterization of frustrated systems, *Physica A* **294**, 180 (2001).
- [34] V. Scarani, M. Ziman, P. Štelmachovič, N. Gisin, and V. Bužek, Thermalizing Quantum Machines: Dissipation and Entanglement, *Phys. Rev. Lett.* **88**, 097905 (2002).
- [35] R. McCloskey and M. Paternostro, Non-Markovianity and system-environment correlations in a microscopic collision model, *Phys. Rev. A* **89**, 052120 (2014).
- [36] N. K. Bernardes, A. R. R. Carvalho, C. H. Monken, and M. F. Santos, Environmental correlations and Markovian to non-Markovian transitions in collisional models, *Phys. Rev. A* **90**, 032111 (2014).
- [37] J. Jin, V. Giovannetti, R. Fazio, F. Sciarrino, P. Mataloni, A. Crespi, R. Osellame, All-optical non-Markovian stroboscopic quantum simulator, *Phys. Rev. A* **91**, 012122 (2015).
- [38] B. Çakmak, M. Pezzutto, M. Paternostro, and Ö. E. Müstecaplıoğlu, Non-Markovianity, coherence, and system-environment correlations in a long-range collision model, *Phys. Rev. A* **96**, 022109 (2017).
- [39] N. K. Bernardes, A. R. R. Carvalho, C. H. Monken, and M. F. Santos, Coarse graining a non-Markovian collisional model, *Phys. Rev. A* **95**, 032117 (2017).
- [40] J. Jin and C.-s. Yu, Non-Markovianity in the collision model with environmental block, *New J. Phys.* **20**, 053026 (2018).
- [41] Z. -X. Man, Y.-J. Xia, and R. L. Franco, Temperature effects on quantum non-Markovianity via collisional models, *Phys. Rev. A* **97**, 062104 (2018).
- [42] S. J. Whalen, Collision model for non-Markovian quantum trajectories, *Phys. Rev. A* **100**, 052113 (2019).
- [43] R. R. Camasca, and G. T. Landi, Memory kernel and divisibility of Gaussian collisional models, *Phys. Rev. A* **103**, 022202 (2021).
- [44] G. Karpat, İ. Yalçınkaya, and B. Çakmak, Quantum synchronization in a collision model, *Phys. Rev. A* **100**, 012133 (2019).
- [45] K. Beyer, K. Luoma, and W. T. Strunz, Collision-model approach to steering of an open driven qubit, *Phys. Rev. A* **97**, 032113 (2018).
- [46] B. Çakmak, S. Campbell, B. Vacchini, Ö. E. Müstecaplıoğlu, and M. Paternostro, Robust multipartite entanglement generation via a collision model, *Phys. Rev. A* **99**, 012319 (2019).
- [47] D. Grimmer, A. Kempf, R. B. Mann, and E. Martín-Martínez, Zeno friction and antifricition from quantum collision models, *Phys. Rev. A* **100**, 042702 (2019).
- [48] P. Strasberg, G. Schaller, T. Brandes, and M. Esposito, Quantum and Information Thermodynamics: A Unifying Framework Based on Repeated Interactions, *Phys. Rev. X* **7**, 021003 (2017).
- [49] L. Li, J. Zou, H. Li, B.-M. Xu, Y.-M. Wang, and B. Shao, Effect of coherence of nonthermal reservoirs on heat transport in a microscopic collision model, *Phys. Rev. E* **97**, 022111 (2018).
- [50] S. Cusumano, V. Cavina, M. Keck, A. De Pasquale, and V. Giovannetti, Entropy production and asymptotic factorization via thermalization: A collisional model approach, *Phys. Rev. A* **98**, 032119 (2018).
- [51] Z.-X. Man, Y.-J. Xia, and R. Lo Franco, Validity of the Landauer principle and quantum memory effects via collisional models, *Phys. Rev. A* **99**, 042106 (2019).
- [52] F. L. S. Rodrigues, G. De Chiara, M. Paternostro, and G.T. Landi, Thermodynamics of Weakly Coherent Collisional Models, *Phys. Rev. Lett.* **123**, 140601 (2019).
- [53] G. O. Alves and G. T. Landi, Bayesian estimation for collisional thermometry, *Phys. Rev. A* **105**, 012212 (2022).
- [54] G. T. Landi, Battery Charging in Collision Models with Bayesian Risk Strategies, *Entropy* **23**, 1627 (2021).
- [55] F. Ciccarello, S. Lorenzo, V. Giovannetti, G. M. Palma, Quantum collision models: open system dynamics from repeated interactions, arXiv: 2106.11974.
- [56] A. Rivas, S. F. Huelga, and M. B. Plenio, Entanglement and Non-Markovianity of Quantum Evolutions, *Phys. Rev. Lett.* **105**, 050403 (2010).
- [57] G. Torre, W. Roga, and F. Illuminati, Non-Markovianity of Gaussian Channels, *Phys. Rev. Lett.* **115**, 070401 (2015).
- [58] D. F. Walls and G. J. Milburn, *Quantum Optics* (Springer, Berlin, 1994).
- [59] P. Marian, T. A. Marian, and H. Scutaru, Distinguishability and nonclassicality of one-mode Gaussian states, *Phys. Rev. A* **69**, 022104 (2004).
- [60] X.-B. Wang, T. Hiroshima, A. Tomita, and M. Hayashi, Quantum information with Gaussian states, *Phys. Rep.* **448**, 1(2007).
- [61] H.-P. Breuer, E.-M. Laine, and J. Piilo, Measure for the Degree of Non-Markovian Behavior of Quantum Processes in Open Systems, *Phys. Rev. Lett.* **103**, 210401 (2009).
- [62] E.-M. Laine, J. Piilo, and H. -P. Breuer, Measure for the non-Markovianity of quantum processes, *Phys. Rev. A* **81**, 062115 (2010).
- [63] A. Serafini, F. Illuminati, and S. De Siena, Symplectic invariants, entropic measures and correlations of Gaussian states, *J Phys. B.* **37**, L21(2004).
- [64] A. Serafini, Multimode Uncertainty Relations and Separability of Continuous Variable States, *Phys. Rev. Lett.* **96**, 110402 (2006).
- [65] C. S. Hamilton, R. Kruse, L. Sansoni, S. Barkhofen, C. Silberhorn, and I. Jex, Gaussian Boson Sampling, *Phys. Rev. Lett.* **119**, 170501 (2017).
- [66] N. Quesada, J. M. Arrazola, and N. Killoran, Gaussian boson sampling using threshold detectors, *Phys. Rev. A* **98**, 062322 (2018).
- [67] R. Kruse, C. S. Hamilton, L. Sansoni, S. Barkhofen, C. Silberhorn, and I. Jex, Detailed study of Gaussian boson sampling,

- Phys. Rev. A. **100**, 032326 (2019).
- [68] H.-S. Zhong, L.-C. Peng, Y. Li, Y. Hu, W. Li, J. Qin, D. Wu, W. Zhang, H. Li, L. Zhang, Z. Wang, L. You, X. Jiang, L. Li, N.-L. Liu, J. P. Dowling, C.-Y. Lu, and J.-W. Pan, Experimental Gaussian Boson sampling, *Sci. Bull.* **64**, 511 (2019).
- [69] A. Crespi, R. Osellame, R. Ramponi, V. Giovannetti, R. Fazio, L. Sansoni, F. De Nicola, F. Sciarrino and P. Mataloni, Anderson localization of entangled photons in an integrated quantum walk, *Nature Photon.* **7**, 322 (2013).
- [70] A. Gerdali, A. Laneve, L. D. Bonavena, L. Sansoni, J. Ferraz, A. Fratalocchi, F. Sciarrino, Á Cuevas, and P. Mataloni, Experimental Investigation of Superdiffusion via Coherent Disordered Quantum Walks, *Phys. Rev. Lett.* **123**, 140501 (2019)
- [71] Y. Lou, S. Liu, and J. Jing, Experimental Demonstration of a Multifunctional All-Optical Quantum State Transfer Machine, *Phys. Rev. Lett.* **126**, 210507 (2021).
- [72] S. Ru, M. An, Y. Yang, R. Qu, F. Wang, Y. Wang, P. Zhang, and F. Li, Quantum state transfer between two photons with polarization and orbital angular momentum via quantum teleportation technology, *Phys. Rev. A* **103**, 052404 (2021).
- [73] J. -D. Lin, W. -Y. Lin, H. -Y. Ku, N. Lambert, Y. -N. Chen, and F. Nori, Quantum steering as a witness of quantum scrambling, *Phys. Rev. A* **104**, 022614 (2021)